First measurement of the asymmetry and the Gerasimov-Drell-Hearn integrand from the $^3\vec{\mathrm{He}}(\vec{\gamma}, p)^2\mathrm{H}$ reaction at an incident photon energy of 29 MeV

G. Laskaris,[1,2,*] W. Ji,[3] X. Yan,[1,2] J. Zhou,[1,2] W. R. Zimmerman,[1,2] M. W. Ahmed,[1,4] T. Averett,[5] A. Deltuva,[6] A. C. Fonseca,[6] H. Gao,[1,2,†] J. Golak,[7] A. Kafkarkou,[1,2,‡] H. J. Karwowski,[1,8] B. Lalremruata,[9] J. Manfredi,[10] J. M. Mueller,[1,2] P. U. Sauer,[11] R. Skibiński,[7] A. P. Smith,[1,2] M. B. Tsang,[10] H. R. Weller,[1,2] H. Witała,[7] Y. K. Wu,[1,2] and Z. W. Zhao[1,2]

[1]*Triangle Universities Nuclear Laboratory, Durham, North Carolina 27708, USA*
[2]*Department of Physics, Duke University, Durham, North Carolina 27708, USA*
[3]*Tsinghua University, Beijing 100084, China*
[4]*Department of Mathematics and Physics, North Carolina Central University, Durham, North Carolina 27707, USA*
[5]*College of William and Mary, Williamsburg, Virginia 23187, USA*
[6]*Centro de Física Nuclear da Universidade de Lisboa, P-1649-003 Lisboa, Portugal*
[7]*M. Smoluchowski Institute of Physics, Jagiellonian University, PL-30059 Kraków, Poland*
[8]*Department of Physics and Astronomy, University of North Carolina at Chapel Hill, Chapel Hill, North Carolina 27599, USA*
[9]*Mizoram University, Aizawl 796004, India*
[10]*NSCL, Michigan State University, East Lansing, Michigan 48824, USA*
[11]*Institut für Theoretische Physik, Leibniz Universität Hannover, D-30167 Hannover, Germany*

(Received 28 October 2020; revised 8 February 2021; accepted 2 March 2021; published 12 March 2021)

The first measurement of the $^3\vec{\mathrm{He}}(\vec{\gamma}, p)^2\mathrm{H}$ process was performed at the High Intensity γ-ray Source (HIγS) facility at Triangle Universities Nuclear Laboratory using a circularly polarized, monoenergetic γ-ray beam and a longitudinally polarized ^{3}He target. The spin-dependent asymmetry and the contribution from the two-body photodisintegration to the ^{3}He Gerasimov-Drell-Hearn integrand are extracted and compared with state-of-the-art three-nucleon system calculations at the incident photon energy of 29 MeV. The data are in general agreement with the various theoretical predictions based on the Siegert theorem or on explicit inclusion of meson-exchange currents.

DOI: 10.1103/PhysRevC.103.034311

I. INTRODUCTION

The study of three-nucleon systems has been of fundamental importance to nuclear physics [1,2] and essential to the study of the partonic structure of the nuclei where the ^{3}He and ^{3}H mirror nuclei are used to extract the ratio of the inelastic structure functions $\frac{F_2^n}{F_2^p}$ [3]. A polarized ^{3}He nucleus is often treated approximately as a polarized neutron because its ground state is dominated by the *S* wave in which the spins of the two protons pair off. Polarized ^{3}He targets have been used for decades to extract the electromagnetic form factors [4–6] and the spin structure functions [7,8] of the neutron, and most recently its three-dimensional structure and dynamics [9]. To extract the neutron information from ^{3}He, corrections for nuclear effects relying on the state-of-the-art three-body calculations need to be applied. Theoretical calculations using Faddeev [10] and Alt-Grassberger-Sandhas equations (AGS) [11] have been carried out for three-body systems using a variety of nucleon-nucleon (NN) potentials [12–14], and three-nucleon forces (3NFs) like Urbana IX (UIX) [15], or CD Bonn + Δ [16]. It is important to test these calculations by experiments which are sensitive to the details of the three-body calculations to help validate the treatment of nuclear effects in extracting information concerning the neutron by employing polarized ^{3}He nuclei. Data from electrodisintegration of polarized ^{3}He [17] were used to test three-body calculations [18], and more recently data from $^3\vec{\mathrm{He}}(\vec{\gamma}, n)pp$ channel at incident photon energies of 12.8, 14.7 and 16.5 MeV were reported [19–22].

Calculations for the two- and three-body photodisintegration of ^{3}He with double polarizations have been carried out by two groups. The calculations by Deltuva *et al.* are based on the AGS version of Faddeev equations and employ the CD Bonn + Δ potential [16] taking into account the corresponding single-baryon and meson-exchange electromagnetic currents (MEC). In photoreactions, i.e., those with real photons, the currents determine the observables through electric and magnetic multipoles with the electric multipoles being more important (except at very low energies). Furthermore, the electric multipoles can be decomposed into lower- and higher-order contributions with the former being the dominant

*gl41@duke.edu
†haiyan.gao@duke.edu
‡Deceased.

one. In the calculations the MEC are included using two approaches: (i) calculating the most important MEC explicitly, however, without achieving a perfect consistency between nuclear forces and currents; (ii) including the dominant part of MEC for electric multipoles implicitly via the Siegert theorem, and the remaining part of MEC explicitly, thereby reducing the MEC-related uncertainty by shifting it to less important terms. Furthermore, the Siegert operator includes also relativistic single-nucleon charge corrections. For these two reasons it is considered as a more complete approach. In both approaches, the results are obtained using the computational technology of Ref. [23] and the proton-proton Coulomb force is taken into account via the method of screening and renormalization [24]. Skibiński *et al.* solve the Faddeev equations by using the AV18 potential [14] and the UIX 3NF [15] with two approaches for MEC: (i) "pion-in-flight" and "seagull" terms—the two dominant components of MEC—are taken into account explicitly [25]; (ii) the dominant MEC contribution to electric multipoles is included implicitly via the Siegert theorem, but only the nonrelativistic single-nucleon current is considered explicitly. Their results are obtained using the computational methods described in Ref. [26]. Note that the approaches based on explicit MEC by both groups have quite similar dynamic content, while in the case of Siegert approaches the included currents are more different. For detailed discussions of various approaches to electromagnetic current operators, see, e.g., review papers [2] and [27].

Another interesting aspect concerning polarized photodisintegration of ^{3}He is related to the Gerasimov-Drell-Hearn (GDH) sum rule [28]. The GDH sum rule relates the energy-weighted difference of the spin-dependent total photoabsorption cross sections for target spin and beam helicity parallel (σ^P) and antiparallel (σ^A) to the anomalous magnetic moment of the target (nuclei or nucleons) as follows:

$$I^{GDH} = \int_{\nu_{thr}}^{\infty} (\sigma^P - \sigma^A)\frac{d\nu}{\nu} = \frac{4\pi^2\alpha}{M^2}\kappa^2 S, \qquad (1)$$

where ν is the photon energy, ν_{thr} is the pion production (two-body breakup) threshold on the nucleon (nucleus), κ is the anomalous magnetic moment, M is the mass, and S is the spin of the nucleon or the nucleus. In ^{3}He and below the pion production threshold, only the two-body and three-body photodisintegration channels contribute to the GDH integral with calculations [23,26] showing that the three-body channel dominates the integrand. The GDH integrand extracted from measurements of the $^3\vec{\mathrm{He}}(\vec{\gamma}, n)pp$ channel at 12.8 and 14.7 MeV [19,20] is in good agreement with theoretical predictions of Ref. [23], and the result at 16.5 MeV [21] is slightly more than one standard deviation higher than the theory.

To fully test the theoretical predictions, not only measurements at higher energies of the three-body breakup channel will be useful. It is also important to test the calculations of two-body breakup channel with double polarizations. A spin-dependent study of $^3\vec{\mathrm{He}}(\vec{\gamma}, p)^2$H reaction together with the $^3\vec{\mathrm{He}}(\vec{\gamma}, n)pp$ channel will provide stringent tests of the modern three-body calculations, and also serve as an important step towards an experimental test of the extended GDH sum rule on the ^{3}He nucleus by combining inclusive electron-scattering measurements above the pion production threshold from other laboratories [29].

Experimentally, the study of $^3\vec{\mathrm{He}}(\vec{\gamma}, p)^2$H reaction is more challenging than the $^3\vec{\mathrm{He}}(\vec{\gamma}, n)pp$ channel, especially at low energies, due to the necessity of detecting low-energy protons. Such protons are detected in a high background environment from other breakup channels from various nuclear species contained in the ^{3}He target wall material. Furthermore, the predicted spin dependence in the $^3\vec{\mathrm{He}}(\vec{\gamma}, p)^2$H reaction cross section is significantly smaller than that of the three-body channel. As such the experimental study of the $^3\vec{\mathrm{He}}(\vec{\gamma}, p)^2$H channel lags behind the corresponding three-body channel.

II. THE EXPERIMENT

In this paper, we present the first measurement of the $^3\vec{\mathrm{He}}(\vec{\gamma}, p)^2$H channel using a longitudinally polarized ^{3}He target and the nearly monoenergetic, ≈100% circularly polarized γ-ray beam of HIγS facility [30] at $\nu = 29$ MeV. The beam intensity on the target was 1–3 × $10^7 \gamma/s$ having an energy spread of 5.0% (FWHM). A 10.56 cm long C_6D_6 cell and two BC-501A-based liquid scintillator neutron detectors placed transverse to the beam direction were utilized to measure the photon flux by detecting the neutrons from the deuteron photodisintegration process. The integrated photon flux was extracted based on the well-known cross sections [31–35].

The experimental apparatus used for this measurement comprised two subsystems: the polarized ^{3}He target and the detector system. The ^{3}He gas target was contained in a one-piece Sol-Gel coated [36] Pyrex® glassware, consisting of a spherical pumping chamber 8.1 cm in diameter and a cylindrical target chamber 39.6 cm long and 2.9 cm in diameter. The two chambers were connected by a transfer tube 0.8 cm in diameter and 9.6 cm long. The target chamber glass thickness was measured by using two independent methods, laser interferometry and an ultrasonic gauge, and it was found to vary from ≈1.1 mm at the center of the target chamber to ≈1.4 mm towards the beam entrance and exit windows. The target was filled with 6.5 ± 0.1 amg of ^{3}He.

The outgoing protons from the ^{3}He photodisintegrations were detected by 72 fully depleted silicon surface barrier detectors. The detectors were placed at the proton angles of 45°, 70°, 95°, and 120° degrees (a total of 18 detectors at each angle). Six aluminum hemispheres were used to place the detectors ≈10 cm away from the center of the ^{3}He target chamber having three hemispheres on each side of the ^{3}He cell target chamber facing each other and creating effectively three smaller target regions from which the protons originated. Each hemisphere housed twelve detectors, four detectors in the horizontal plane, four detectors above, and four below the horizontal plane covering for each plane all aforementioned angles. Collimators with rectangular apertures of 2 cm × 0.4 cm and a length of 3 cm were placed in front of the detectors. The detector thicknesses ranged from 300 to 500 μm, and their efficiency for detecting charged particles was 100%.

The spin-exchange optical pumping technique [37] was used to polarize ^{3}He target. A small quantity of Rb and K mixture was placed inside the pumping chamber which was heated to 196 °C. A circularly polarized 794.8 nm laser light incident on the pumping chamber polarized Rb atoms which in turn transferred their polarization to ^{3}He nuclei through spin-exchange collisions between Rb-K, Rb-^{3}He, and K-^{3}He. A small quantity of N_2 (0.1 amg) was added into the cell as a buffer gas to improve the optical pumping efficiency. A pair of Helmholtz coils ≈170 cm in diameter providing a 20 G magnetic field was used to define the direction of the ^{3}He nuclear polarization. The spin of the target was flipped every 15 min. The nuclear magnetic resonance-adiabatic fast passage [38] calibrated by the electron paramagnetic resonance technique [39] was employed to measure the absolute target polarization. While a polarization over 40% from target named "SPOT" was achieved in the three-body photodisintegration experiment [19,20] and a 35% polarization in a follow-up experiment [21], for this two-body breakup measurement the polarization of the target was measured to be 33% for the initial run period (≈40% of the beam time) and 22% for the final runs (≈60% of the beam time) due to some hardware failure during the experiment. More details about this target can be found in Refs. [22,40,41].

A N_2-only reference cell with the same dimensions as those of the ^{3}He target chamber was filled with the same amount of N_2 gas and placed right below the ^{3}He target to measure backgrounds. In addition to N_2, backgrounds mainly originated from the entrance and exit windows of the target chamber, which were suppressed by the collimators mounted in front of the detectors and from its side-wall. A lead wall with a 16 mm aperture allowing for the γ beam to pass was placed in front of the targets and the detector system to attenuate the beam halo and reduce background from the side-wall and the electron background from Compton scattering. Figure 1 shows a schematic view of the experimental apparatus including the polarized ^{3}He target subsystem, the 72-detector subsystem, and the C_6D_6 flux monitor.

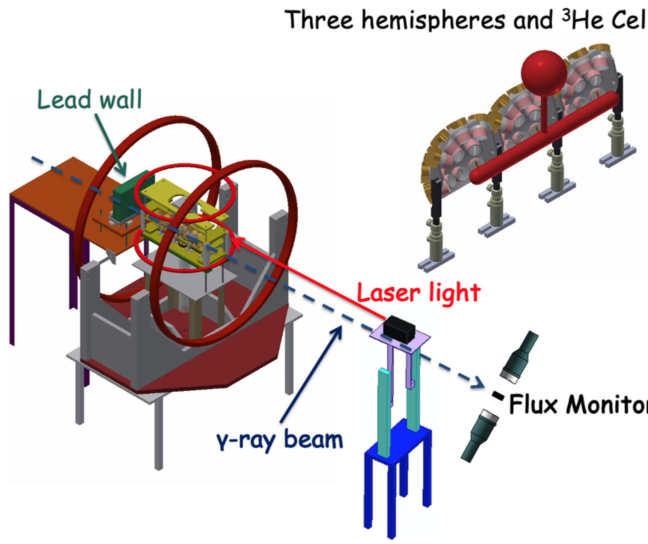

FIG. 1. A view of the experimental apparatus (not to scale). The movable target system, moving up and down to cycle between the ^{3}He cell and the N_2 reference cell for performing signal and background measurements, is surrounded by 72 silicon surface barrier detectors. Half of the detector system (three hemispheres supporting 36 detectors shown here for clarity) and the ^{3}He cell can be seen at the top right. The lead wall placed in front of the targets and the detector system can be seen at the left. The movable support of the laser system used to polarize ^{3}He can be seen next to the C_6D_6 flux monitor at the right.

III. DATA ANALYSIS AND RESULTS

Two quantities were recorded for each event, the incident charged particle energy E_p and the relative time of flight (TOF) between the silicon detectors and the rf signal of the beam. A two-dimensional cut was applied to the energy plotted against the relative TOF and used to select the protons from the ^{3}He cell. The same cuts were applied to the data taken with the N_2 reference cell to subtract the proton background from other processes. Figure 2 shows the two-dimensional histogram of the TOF plotted versus the E_p. The protons from the competing $^3\vec{\mathrm{He}}(\vec{\gamma}, p)pn$ reaction could not be subtracted using the N_2 reference cell. A GEANT4 [42] simulation using the measured glass thicknesses of the target chamber, taking into account all the physical volumes surrounding the ^{3}He cell, the detector technical characteristics, and responses has shown that no protons from the three-body photodisintegration of ^{3}He can make it into the detectors.

After selecting the protons, the spin-dependent asymmetry for each detector can be formed as

$$A = \frac{1}{P_b P_t} \frac{Y^P - Y^A}{Y^P + Y^A}, \qquad (2)$$

where P_b and P_t are the beam and target polarization, respectively, and $Y^{P/A}$ are the integrated normalized yields (proton counts per integrated photon flux) with $Y^{P/A} = Y^{P/A,^3\mathrm{He}} - Y^{N_2}$ being the measured yield from the ^{3}He cell after the subtraction of the N_2 reference cell background yield for both parallel and antiparallel states. Although the uneven glass thickness of the ^{3}He target chamber affected the proton yields for each detector, it did not affect the asymmetry, as shown by the GEANT4 simulation of the experiment. This allowed the calculation of the asymmetry for each angle as the weighted

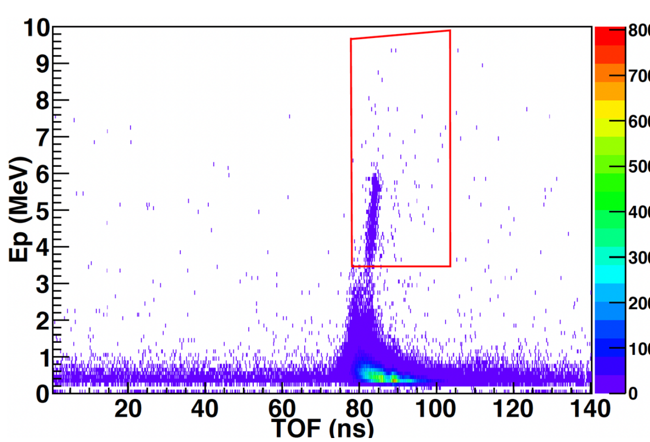

FIG. 2. The TOF versus Ep spectrum for a detector at 95 °. The protons were chosen by applying a two-dimensional cut indicated by a red curve and are well separated from the electrons.

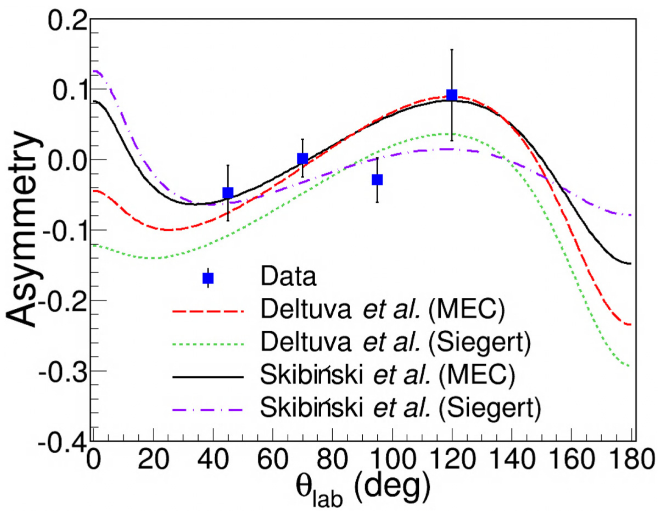

FIG. 3. Measured spin-dependent asymmetry including statistical and systematic uncertainties compared with the calculations of Deltuva *et al.* [23] and Skibiński *et al.* [26] at $\nu = 29$ MeV.

average of the asymmetries of all 18 detectors at this angle. By forming the asymmetry for each detector, many systematic uncertainties including those associated with the solid angle and the detector efficiency were canceled. Still, there were two remaining contributions to the systematic uncertainty, namely, the target polarization of 4.2% and the beam polarization of 1.0%, which resulted in an overall relative systematic uncertainty of 4.3%.

The measured spin-dependent asymmetries as a function of the proton-scattering angle, θ_{lab} at $\nu = 29$ MeV are shown in Fig. 3 including statistical and systematic uncertainties added in quadrature. The data are compared with the two sets of theoretical calculations provided by Deltuva *et al.* [23] and Skibiński *et al.* [26]. Although the calculations based on the Siegert theorem with relativistic charge corrections are considered to be more complete, the overall shape of the experimental results seem to be described better by the calculations taking into account the MEC explicitly. However, one cannot reach a definitive conclusion as to which theoretical calculation is favored by the asymmetry data given the overall uncertainties.

By combining the measured asymmetry, the known angular distribution of the unpolarized differential cross sections [43] and the total cross sections [44,45] at 29 MeV, one can extract the spin-dependent differential cross sections. Second-order Legendre polynomials are used to fit the spin-dependent differential cross sections and the fitting curves are integrated over the angle to extract the spin-dependent total cross sections and the GDH integrand.

Table I summarizes the extracted spin-dependent total cross sections and the contribution from the two-body photodisintegration to the ^{3}He GDH integrand in comparison to the two sets of calculations from Deltuva *et al.* [23] and Skibiński *et al.* [26]. The reported uncertainties include the statistical and systematic uncertainties of the current asymmetry measurement and the uncertainties associated with the known angular distribution [43] and the total cross sections [44,45].

TABLE I. The extracted spin-dependent total cross sections, σ^P and σ^A, and the contributions from the two-body photodisintegration to ^{3}He GDH integrand, $(\sigma^P - \sigma^A)/\nu$ compared with theoretical predictions.

	$\sigma^P(\mu\text{b})$	$\sigma^A(\mu\text{b})$	$(\sigma^P - \sigma^A)/\nu$ (fm^3)
This work	277 ± 32	276 ± 30	$(0.07 \pm 2.77) \times 10^{-2}$
Deltuva *et al.* (MEC)	305	306	-6.8×10^{-4}
Deltuva *et al.* (Siegert)	309	336	-1.84×10^{-2}
Skibiński *et al.* (MEC)	303	299	2.72×10^{-3}
Skibiński *et al.* (Siegert)	295	310	-1.02×10^{-2}

The extracted spin-dependent total cross sections are slightly smaller in magnitude but within $\approx 1\sigma$ from the calculations. As expected based on the asymmetry results, the extracted GDH integrand seems to favor the explicit MEC-based calculations.

Figure 4 shows the contributions from two-body photodisintegration to the ^{3}He GDH integrand together with the two sets of predictions from Deltuva *et al.* [23] and Skibiński *et al.* [26] as a function of the incident photon energy. In the same figure the past measurements of the contributions from the three-body photodisintegration to the ^{3}He GDH integrand together with the predictions from Refs. [23] and [26] are shown for comparison. The dominance of the three-body over the two-body photodisintegration contribution to the GDH integrand might be explained by the much larger total three-body cross sections than that of the two-body channel in this energy range. Noteworthy, the best description of two- and three-body data is given by different calculations, based either on explicit MEC or Siegert with relativistic charge corrections, respectively.

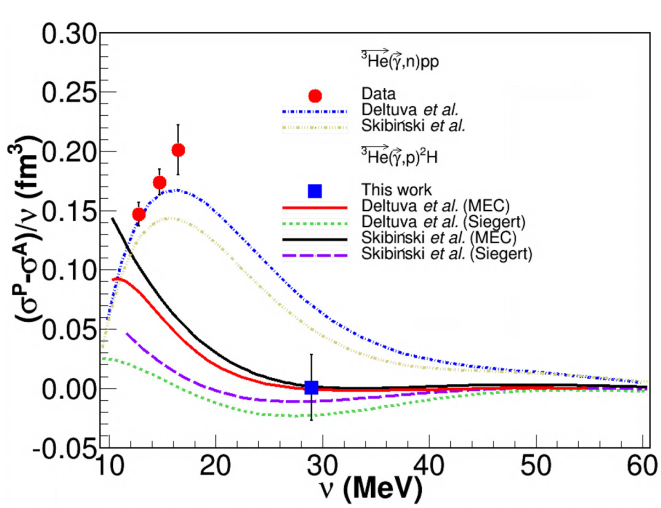

FIG. 4. The extracted GDH integrand of $^3\vec{\text{He}}(\vec{\gamma}, p)^2\text{H}$ (blue square) plotted together with the results from $^3\vec{\text{He}}(\vec{\gamma}, n)pp$ (red circles) [19–22] including statistical and systematic uncertainties compared with the calculations of Deltuva *et al.* [23] and Skibiński *et al.* [26].

IV. SUMMARY AND CONCLUSIONS

In this paper, we report the first measurement of the double polarized $^3\vec{\text{He}}(\vec{\gamma}, p)^2\text{H}$ reaction. It is remarkable to note that the new data and the previous data on the three-body channel support the theoretical predictions of the dominance of the $^3\vec{\text{He}}(\vec{\gamma}, n)pp$ channel over the $^3\vec{\text{He}}(\vec{\gamma}, p)^2\text{H}$ channel in the contribution to the ^{3}He GDH integrand below the pion production threshold. Providing additional data for the observables sensitive to the details of exchange currents is important in view of future analysis with chiral currents. These additional data, when combined with data from three-body photodisintegration and data above the pion production threshold from other laboratories, will directly test the theoretical calculations and the ^{3}He GDH sum-rule predictions. On the theory front, supplementing the currents used with terms allowing to fulfill the continuity equation should significantly improve agreement between the predictions presented in this paper. The ongoing efforts to construct such complete electromagnetic currents consistent with the chiral interaction give hope for future studies of the influence of the current conservation breaking on photodisintegration observables.

ACKNOWLEDGMENTS

We would like to thank M. Souza and G. Cates for their assistance in constructing the Sol-Gel coated cell and the TUNL personnel, in particular, the HIγS operation team for the technical support of this experiment. This work is supported by the U.S. Department of Energy under Contracts No. DE-FG02-03ER41231, No. DE-FG02-97ER41033, No. DE-FG02-97ER41041, No. DE-SC0005367, the US National Science Foundation under Contract No. PHY-1565546, and the Polish National Science Center under Grant No. 2016/22/M/ST2/00173. A.D. acknowledges support by the Alexander von Humboldt Foundation under Grant No. LTU-1185721-HFST-E. The numerical calculations of Kraków theoretical group have been performed on the supercomputer clusters of the JSC, Jülich, Germany.

[1] W. Glöckle, H. Witała, D. Hüber, H. Kamada, and J. Golak, Phys. Rep. **274**, 107 (1996).
[2] J. Carlson and R. Schiavilla, Rev. Mod. Phys. **70**, 743 (1998).
[3] H. Liu, Ph.D. thesis, Columbia University, 2020 (unpublished).
[4] H. Gao, J. Arrington, E. J. Beise, B. Bray, R. W. Carr, B. W. Filippone *et al.*, Phys. Rev. C **50**, R546 (1994).
[5] W. Xu *et al.*, Phys. Rev. Lett. **85**, 2900 (2000).
[6] S. Riordan *et al.*, Phys. Rev. Lett. **105**, 262302 (2010).
[7] P. L. Anthony, R. G. Arnold, H. R. Band, H. Borel, P. E. Bosted, V. Breton *et al.*, Phys. Rev. D **54**, 6620 (1996).
[8] X. Zheng *et al.* (Jefferson Lab Hall A Collaboration), Phys. Rev. Lett. **92**, 012004 (2004); X. Zheng *et al.*, Phys. Rev. C **70**, 065207 (2004).
[9] X. Qian *et al.* (Jefferson Lab Hall A Collaboration), Phys. Rev. Lett. **107**, 072003 (2011).
[10] L. D. Faddeev, Zh. Eksp. Teor. Fiz. **39**, 1459 (1961) [Sov. Phys. JETP **12**, 1014 (1961)].
[11] E. O. Alt, P. Grassberger, and W. Sandhas, Nucl. Phys. B **2**, 167 (1967).
[12] V. G. J. Stoks, R. A. M. Klomp, C. P. F. Terheggen, and J. J. deSwart, Phys. Rev. C **49**, 2950 (1994).
[13] R. Machleidt, Phys. Rev. C **63**, 024001 (2001).
[14] R. B. Wiringa, V. G. J. Stoks, and R. Schiavilla, Phys. Rev. C **51**, 38 (1995).
[15] B. S. Pudliner, V. R. Pandharipande, J. Carlson, S. C. Pieper, and R. B. Wiringa, Phys. Rev. C **56**, 1720 (1997).
[16] A. Deltuva, R. Machleidt, and P. U. Sauer, Phys. Rev. C **68**, 024005 (2003).
[17] F. Xiong *et al.*, Phys. Rev. Lett. **87**, 242501 (2001).
[18] J. Golak, R. Skibiński, H. Witała, W. Glöckle, A. Nogga, and H. Kamada, Phys. Rep. **415**, 89 (2005).
[19] G. Laskaris, Q. Ye, B. Lalremruata, Q. J. Ye, M. W. Ahmed, T. Averett *et al.*, Phys. Rev. Lett. **110**, 202501 (2013).
[20] G. Laskaris, Q. Ye, B. Lalremruata, Q. J. Ye, M. W. Ahmed, T. Averett *et al.*, Phys. Rev. C **89**, 024002 (2014).
[21] G. Laskaris, X. Yan, J. M. Mueller, W. R. Zimmerman, W. Xiong, M. W. Ahmed *et al.*, Phys. Lett. B **750**, 547 (2015).
[22] G. Laskaris, Ph.D. thesis, Duke University, 2015 (unpublished).
[23] A. Deltuva, L. P. Yuan, J. Adam, A. C. Fonseca, and P. U. Sauer, Phys. Rev. C **69**, 034004 (2004); A. Deltuva, A. C. Fonseca, and P. U. Sauer, *ibid.* **71**, 054005 (2005); **72**, 054004 (2005); **80**, 064004 (2009).
[24] A. Deltuva, A. C. Fonseca, and P. U. Sauer, Annu. Rev. Nucl. Part. Sci. **58**, 27 (2008).
[25] J. Golak, H. Kamada, H. Witała, W. Glöckle, J. Kuros, R. Skibiński, V. V. Kotlyar, K. Sagara, and H. Akiyoshi, Phys. Rev. C **62**, 054005 (2000).
[26] R. Skibiński, J. Golak, H. Kamada, H. Witała, W. Glöckle, and A. Nogga, Phys. Rev. C **67**, 054001 (2003); R. Skibiński, J. Golak, H. Witała, W. Glöckle, A. Nogga, and H. Kamada, *ibid.* **72**, 044002 (2005); R. Skibiński, J. Golak, H. Witała, W. Glöckle, and A. Nogga, Eur. Phys. J. A **24**, 31 (2005).
[27] S. Bacca and S. Pastore, J. Phys. G **41**, 123002 (2014).
[28] S. D. Drell and A. C. Hearn, Phys. Rev. Lett. **16**, 908 (1966); S. B. Gerasimov, Yad. Fiz. **2**, 598 (1965) [Sov. J. Nucl. Phys. **2**, 430 (1966)].
[29] M. Amarian *et al.*, Phys. Rev. Lett. **89**, 242301 (2002).
[30] H. R. Weller, M. W. Ahmed, H. Gao, W. Tornow, Y. K. Wu, M. Gai, and R. Miskimen, Prog. Part. Nucl. Phys. **62**, 257 (2008).
[31] R. Bernabei, A. Incicchitti, M. Mattioli, P. Picozza, D. Prosperi, L. Casano *et al.*, Phys. Rev. Lett. **57**, 1542 (1986).
[32] M. A. Blackston, Ph.D. thesis, Duke University, 2007 (unpublished).
[33] Y. Birenbaum, S. Kahane, and R. Moreh, Phys. Rev. C **32**, 1825 (1985).
[34] A. De Graeve, R. Van de Vyver, A. Zieger, C. Van den Abeele, L. Van Hoorebeke, D. Ryckbosch, H. Ferdinande, F. De Smet, B. Ziegler, P. Wilhelm, and H. Arenhövel, Phys. Rev. C **45**, 860 (1992).

[35] D. M. Skopik, Y. M. Shin, M. C. Phenneger, and J. J. Murphy, II, Phys. Rev. C **9**, 531 (1974).
[36] C. Brinker, *Sol-Gel Science* (Academic Press, 1990).
[37] W. Happer, Rev. Mod. Phys. **44**, 169 (1972).
[38] W. Lorenzon, T. R. Gentile, H. Gao, and R. D. McKeown, Phys. Rev. A **47**, 468 (1993).
[39] M. V. Romalis and G. D. Cates, Phys. Rev. A **58**, 3004 (1998), and references therein.
[40] K. Kramer, X. Zong, D. Dutta, H. Gao, X. Qian, Q. Ye, X. Zhu, R. Lu, T. Averett, and S. Fuchs, Nucl. Instrum. Methods Phys. Res., Sect. A **582**, 318 (2007).
[41] Q. Ye, G. Laskaris, W. Chen, H. Gao, W. Zheng, X. Zong, T. Averett, G. D. Cates, and W. A. Tobias, Eur. Phys. J. A **44**, 55 (2010).
[42] S. Agostinelli *et al.*, Nucl. Instrum. Methods Phys. Res., Sect. A **506**, 250 (2003).
[43] M. Anghinolfi, P. Corvisiero, M. Guarnone, G. Ricco, and A. Zucchiatti, Nucl. Phys. A **410**, 173 (1983).
[44] S. K. Kundu, Y. M. Shin, and G. D. Wait, Nucl. Phys. A **171**, 384 (1971).
[45] G. Ticcioni, S. N. Gardiner, J. L. Matthews, and R. O. Owens, Phys. Lett. B **46**, 369 (1973).